Since January 2020 Elsevier has created a COVID-19 resource centre with free information in English and Mandarin on the novel coronavirus COVID-19. The COVID-19 resource centre is hosted on Elsevier Connect, the company's public news and information website.

Journal of Cardiothoracic and Vascular Anesthesia 35 (2021) 3631–3641

Contents lists available at ScienceDirect

Journal of Cardiothoracic and Vascular Anesthesia

journal homepage: www.jcvaonline.com

Original Article

Pulmonary Vascular Thrombosis in COVID-19 Pneumonia

Francesco De Cobelli, MD[*,†], Diego Palumbo, MD[*,†], Fabio Ciceri, MD[*,‡], Giovanni Landoni, MD[*,§,1], Annalisa Ruggeri, MD[‡], Patrizia Rovere-Querini, MD[*,**], Armando D'Angelo, MD[*,¶], Stephanie Steidler[†], Laura Galli[‖], Andrea Poli[‖], Evgeny Fominskiy, MD[§], Maria Grazia Calabrò, MD[§], Sergio Colombo, MD[§], Giacomo Monti, MD[§], Roberto Nicoletti, MD[†], Antonio Esposito, MD[*,†], Caterina Conte, MD[*,**], Lorenzo Dagna, MD[*,#], Alberto Ambrosio, MD[***], Paolo Scarpellini, MD[‖], Marco Ripa, MD[‖], Marzia Spessot, MD[††], Michele Carlucci, MD[‡‡], Matteo Montorfano, MD[¶¶], Eustachio Agricola, MD[*,##], Domenico Baccellieri, MD[§§], Emanuele Bosi, MD[*,****], Moreno Tresoldi, MD[††], Antonella Castagna, MD[*,‖], Gianvito Martino, MD[*,‖‖], Alberto Zangrillo, MD[*,§]

[*]*Vita-Salute San Raffaele University, Milan, Italy*
[†]*Radiology Department, Experimental Imaging Center, IRCCS San Raffaele Scientific Institute, Milan, Italy*
[‡]*Hematology and Bone Marrow Transplantation, IRCCS San Raffaele Scientific Institute, Milan, Italy*
[§]*Department of Anesthesia and Intensive Care, IRCCS San Raffaele Scientific Institute, Milan, Italy*
[**]*Division of Immunology, Transplantation and Infectious Diseases, IRCCS San Raffaele Scientific Institute, Milan, Italy*
[‖]*Unit of Infectious Diseases, IRCCS, San Raffaele Scientific Institute, Milan, Italy*
[¶]*Coagulation Service and Thrombosis Research Unit, IRCCS San Raffaele Scientific Institute, Milan, Italy*
[#]*Unit of Immunology, Rheumatology, Allergy, and Rare Diseases (UnIRAR), IRCCS San Raffaele Scientific Institute, Milan, Italy*
[***]*Clinical Governance, IRCCS San Raffaele Scientific Institute, Milan, Italy*
[††]*Unit of General Medicine and Advanced Care, IRCCS San Raffaele Scientific Institute, Milan, Italy*
[‡‡]*Emergency Department, IRCCS San Raffaele, Milan, Italy*
[¶¶]*Interventional Cardiology Unit, IRCCS San Raffaele Scientific Institute, Milan, Italy*
[##]*Cardiovascular Imaging Unit, Cardio-Thoracic-Vascular Department, IRCCS San Raffaele Scientific Institute, Milan, Italy*
[§§]*Cardio-Thoracic-Vascular Department, San Raffaele Scientific Institute, Milan, Italy*

Author's contribution: All authors contributed to conception, data collection, data analysis, and manuscript writing.

Funding: None.

Collaborators to be added in PubMed and Scopus (all from San Raffaele Scientific Institute): Daniele Grippaldi, MD, Roberta Cao, MD, Stefania Calvisi, MD, Valentina Da Prat, MD, Raffaella Scotti, MD, Giorgia Borio, MD, Ludovica Cavallo, MD, Jacopo Castellani, MD, Federica Farolfi, MD, Maria Pascali MD, Diana Canetti, MD, Barbara Castiglioni, MD, Chiara Oltolini, MD, Chiara Tassan Din, MD, Anna Mara Scandroglio, MD, Marianna Sartorelli, MD, Alessandro Belletti, MD, Pasquale Nardelli, MD, Alessandro Ortalda, MD, Gaetano Lombardi, MD, Federica Morselli, MD, Ottavia Pallanch, MD, Carolina Faustini, MD.

[1]Address correspondence to Giovanni Landoni, MD, Department of Anesthesia and Intensive Care, IRCCS San Raffaele Scientific Institute, Via Olgettina 60, Milano, 20132 Italy.

E-mail address: landoni.giovanni@hsr.it (G. Landoni).

https://doi.org/10.1053/j.jvca.2021.01.011

[****]Unit of General Medicine, Endocrine and Metabolic Diseases, IRCCS San Raffaele Scientific Institute, Milan, Italy
[IIII]Division of Neuroscience, Institute of Experimental Neurology, IRCCS San Raffaele Scientific Institute, Milan, Italy

Objectives: During severe acute respiratory syndrome coronavirus 2 (SARS-CoV-2) infection, dramatic endothelial cell damage with pulmonary microvascular thrombosis have been was hypothesized to occur. The aim was to assess whether pulmonary vascular thrombosis (PVT) is due to recurrent thromboembolism from peripheral deep vein thrombosis or to local inflammatory endothelial damage, with a superimposed thrombotic late complication.
Design: Observational study.
Setting: Medical and intensive care unit wards of a teaching hospital.
Participants: The authors report a subset of patients included in a prospective institutional study (CovidBiob study) with clinical suspicion of pulmonary vascular thromboembolism.
Interventions: Computed tomography pulmonary angiography and evaluation of laboratory markers and coagulation profile.
Measurements and Main Results: Twenty-eight of 55 (50.9%) patients showed PVT, with a median time interval from symptom onset of 17.5 days. Simultaneous multiple PVTs were identified in 22 patients, with bilateral involvement in 16, mostly affecting segmental/subsegmental pulmonary artery branches (67.8% and 96.4%). Patients with PVT had significantly higher ground glass opacity areas (31.7% [22.9-41] *v* 17.8% [10.8-22.1], $p < 0.001$) compared with those without PVT. Remarkably, in all 28 patients, ground glass opacities areas and PVT had an almost perfect spatial overlap. D-dimer level at hospital admission was predictive of PVT.
Conclusions: The findings identified a specific radiologic pattern of coronavirus disease 2019 (COVID-19) pneumonia with a unique spatial distribution of PVT overlapping areas of ground-glass opacities. These findings supported the hypothesis of a pathogenetic relationship between COVID-19 lung inflammation and PVT and challenged the previous definition of pulmonary embolism associated with COVID-19 pneumonia.

Key Words: COVID-19; thrombosis; D-dimer increase; inflammation; critical care; computed tomography

CLINICAL MANIFESTATIONS of coronavirus disease 2019 (COVID-19) include a variety of phenotypes, spanning from asymptomatic disease to severe interstitial pneumonia with acute respiratory distress syndrome (ARDS) and death. The clinical evolution of COVID-19 can be described in three major patterns[1]: mild illness with upper respiratory tract clinical symptoms; non-life-threatening pneumonia; and severe pneumonia with ARDS, which begins with mild symptoms for seven-to-eight days and then rapidly progresses to symptoms requiring advanced life support.

In addition to a possible direct cytopathic effect, the virus may elicit a local cytokine-dependent inflammatory and potentially detrimental immune reaction. The authors previously hypothesized that this host immune response may cause massive vascular endothelial and alveolar epithelial cell damage, with microvascular thrombosis leading to worsening of ventilation/perfusion imbalances and loss of hypoxic vasoconstrictor reflexes.[2] Progression of this endothelial thrombo-inflammatory syndrome to the microvascular bed of other vital organs may result in multiple organ failure and, eventually, death. Direct viral infection of the endothelial cells, with diffuse endothelial inflammation, and apoptosis has been reported in kidney, small bowel, and lung tissue specimens from patients with COVID-19.[3] On the other hand, pulmonary embolism has been described as part of the clinical manifestation associated with COVID-19 pneumonia,[4-6] as have elevated D-dimers.[6-8] In this peculiar pathogenic scenario, it could be argued whether pulmonary vascular thrombosis is due to recurrent thromboembolism from peripheral deep vein thrombosis (DVT) or rather to local inflammatory endothelial damage with a superimposed thrombotic late complication.

A possible hint to such a pathogenic dilemma could come from imaging. Computed tomography (CT) pulmonary angiography is a noninvasive imaging tool able to identify filling defects in pulmonary artery branches,[9] as well as radiologic hallmarks of COVID-19 pneumonia: bilateral ground-glass opacities (GGOs), crazy paving pattern, and/or consolidations predominantly in subpleural locations in the lower lobes.[10,11] Furthermore, chest CT (irrespective of contrast medium administration) has been used to quantify disease burden.[12,13]

To address the question of whether pulmonary vascular thrombosis reflects recurrent thromboembolism from peripheral DVT or rather local thrombosis secondary to inflammatory endothelial damage, along with inflammatory markers and coagulation profile, spatial distribution of pulmonary vascular thrombosis in severe acute respiratory syndrome coronavirus 2 (SARS-CoV-2) pneumonia was evaluated in a consecutive cohort of patients with COVID-19 with clinical suspicion of pulmonary thromboembolism. Specifically, the topographic pattern of distribution of pulmonary vascular thrombosis was investigated using CT pulmonary angiography and then correlated with pneumonia extent.

Methods

This series was a subset of a larger prospective study at the San Raffaele Scientific Institute, a 1,350-bed tertiary care academic hospital in Milan, Italy; the COVID-BioB study is an institutional observational study with the aim to collect and analyze biologic samples and clinical outcomes in patients with COVID-19 (COVID-BioB, ClinicalTrials.gov NCT04318366). The study

was approved by the institutional review board (protocol number 34/INT/2020). All procedures were conducted in agreement with the Declaration of Helsinki (1,964 and further amendments); informed consent was collected from all patients according to the institutional review board guidelines.

Between March 29 and April 9, 2020, patients with a positive nasopharyngeal swab result for SARS-CoV-2, who underwent CT pulmonary angiography for clinical suspicion of pulmonary vascular thrombosis, were enrolled in this study. Last follow-up date was set at July 15, 2020. Clinical suspicion of pulmonary vascular thrombosis in patients with SARS-CoV 2 was defined as ARDS nonresponsive to increasing O_2 therapy.

Exclusion criteria were defined as (1) severe respiratory and/or motion artifacts that did not allow proper evaluation of lung parenchyma and identification of eventual filling defects in pulmonary arteries branches, and (2) pneumothorax (Fig 1).

Clinical Data Collection

Data were entered into a dedicated electronic case report form specifically developed on site for the COVID-BioB study. Before analysis, data managers and clinicians verified data for accuracy. Details regarding treatments administered to patients other than anticoagulants previously have been reported extensively by the authors' group.[14] Data regarding lower- and upper-limb compression ultrasonography with Doppler evaluation also were collected to evaluate possible DVT.

CT Protocol

CT pulmonary angiography examinations first were performed in a dedicated CT suite (GE CT Light Speed VCT CardiacPro), easily accessible via assigned elevators and paths from the emergency department, SARS-CoV-2-dedicated intensive care units (ICUs), and COVID-dedicated wards.[15] Two additional ICUs specifically dedicated to critically ill COVID-19 patients, with a total of 24 beds, were created with a dedicated novel CT scanner (Philips CT Incisive 128 pro).[15]

CT pulmonary angiography protocol included an unenhanced, breath-hold axial scan of the thorax (from lung apex to the lowest hemidiaphragm), followed by an additional scan starting a few seconds after intravenous administration of nonionic iodinate contrast medium to specifically enhance pulmonary arteries and their branches; the automatic bolus tracking technique had the region of interest positioned in the right ventricle, with a trigger threshold of 100 Hounsfield units (HU). This protocol ensured evaluation of lung parenchyma and eventual filling defects in the branches of the pulmonary arteries because an enhanced scan alone would not allow proper characterization of pneumonia.[16]

Image Evaluation

All CT pulmonary angiography images were reviewed independently by two radiologists experienced in thoracic imaging (R.N. and D.P., with 28 and five years of experience, respectively) both blinded to the patient symptoms and outcome; differences in assessment were resolved with consensus. Pulmonary vascular thrombosis was defined when contrast-enhanced CT demonstrated filling defects in the branches of the pulmonary arteries and classified in distribution (number and site of pulmonary lobes affected) and extent (down to subsegmental branches). Irrespective of presence or absence of pulmonary vascular thrombosis, the diameter of perilesional subsegmental vessels always

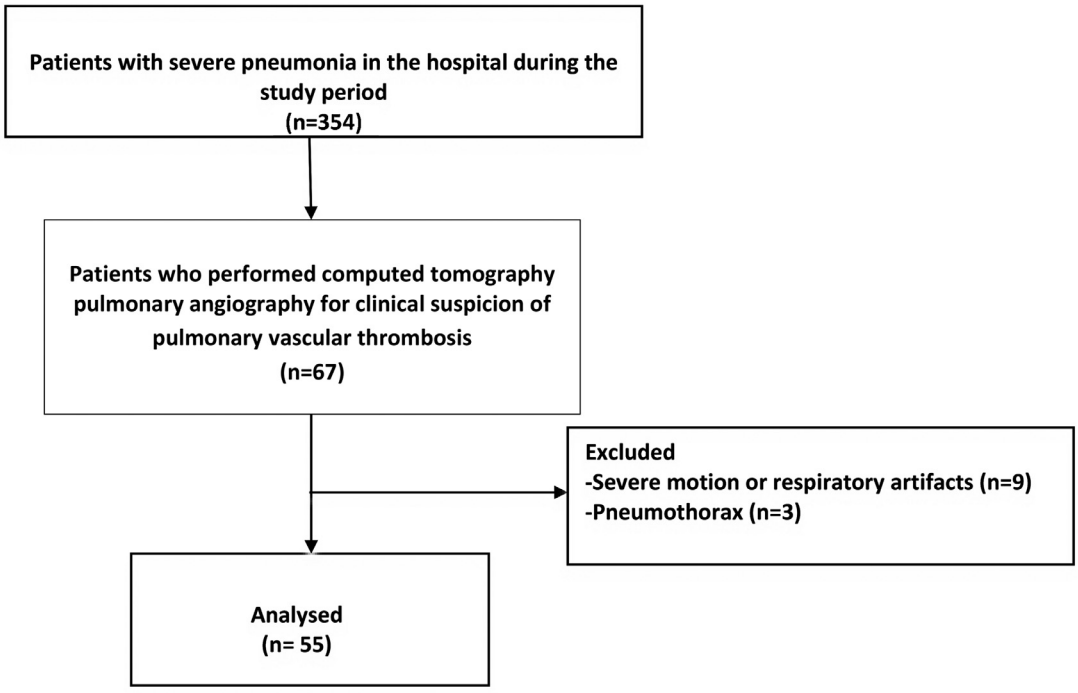

Fig 1. Flowchart of the study.

Table 1
Baseline Characteristics of the 55 Patients With COVID-19 Who Had a Computerized Tomography Pulmonary Angiography Scan Performed at the Institute

Characteristics (%)	Overall, n = 55	Without Pulmonary Vascular Thrombosis (n=27)	With Pulmonary Vascular Thrombosis (n=28)	p Value*
Age, y (IQR)	62 (56-71)	62 (56-74)	62 (54.5-68)	0.76
Sex, M	39 (72)	19 (73)	20 (71)	0.89
Ethnicity				
White	47 (85)	20 (74)	27 (96)	
Asian	8 (15)	7 (26)	1 (4)	0.02
Onset of COVID-19 symptoms, d	17.5 (10-23)	19 (10-25)	14 (9-22)	0.17
Body temperature ˚C	37.6 (36.5-38.3)	38 (37- 38.7)	37.4 (36- 38.2)	0.07
$PaO2/F_IO_2$ ratio	247 (106.7-307)	252 (91-310)	247 (121-307)	0.96
BMI kg/m^2	26 (25-31)	25 (24-29)	28(25-34)	0.14
Presence of comorbidities	27 (52.9)	11 (45.8)	16 (59.3)	0.33
Hypertension				0.84
No	29 (56.9)	14 (58.3)	15 (56)	
Yes	22 (43.1)	10 (41.7)	12 (44)	
Coronary artery disease				0.69
No	44 (86.3)	20 (83)	24 (89)	
Yes	7 (13.7)	4 (17)	3 (11)	
Diabetes				0.58
No	40 (78)	19 (79)	21 (78)	
Yes	11 (22)	5 (21)	6 (22)	
COPD				0.64
No	47 (92)	22 (91.7)	25 (92.6)	
Yes	4 (8)	2 (8.3)	2 (7.4)	
Chronic kidney disease				0.47
No	50 (98)	23 (88.2)	27 (100)	
Yes	1 (2)	1 (11.8)	0	
Cancer				0.52
No	50 (98)	24 (100)	26 (96)	
Yes	1 (2)	0	1 (4)	
Neurodegenerative disorders				0.49
No	52 (97.1)	25 (97.1)	27 (100)	
Yes	1 (2.9)	1 (2.9)	0	
WBC, $\times 10^9$/L	9.0 (6.3-12.3)	9.2 (6.0-12.8)	8.90 (6.52-12.15)	0.78
Missing	0	0	0	
Lymphocyte count, $\times 10^9$/L	0.8 (0.7-1.2)	0.9 (0.7-1.2)	0.8 (0.7-1.2)	0.83
Missing	3	2	1	
Neutrophil count, $\times 10^9$/L	7.5 (4.9-10.0)	7.90 (4.65-10.65)	6.8 (4.9-9.9)	0.57
Missing	3	2	1	
Hemoglobin, g/dL	13.5 (12.3-14.6)	13 (11.5-14.2)	13.6 (13.0-14.8)	0.08
Missing	0	0	0	
Platelet count, $\times 10^9$/L	247 (194-372)	248 (214-430)	247 (170-328)	0.27
Missing	6	3	3	
Albumin, g/L	25.4 (23.6-28.2)	26.0 (22.6-28.2)	25.3 (23.7-28.3)	0.9
Missing	11	4	7	
ALT, U/L	50 (31-73)	49 (27-67)	50 (32-83)	0.66
Missing	6	3	3	
AST, U/L	58 (45-78)	59 (47-79)	57 (36-87)	0.52
Missing	7	4	3	
Creatinine, mg/dL	10 (0.84-1.19)	0.99 (0.88-1.09)	11 (0.81-1.20)	0.57
Missing	0	0	0	
Glucose, mg/dL	109 (97-151)	117 (92-154)	106 (99-146)	0.54
Missing	3	1	2	
Lactate dehydrogenase, U/L	490 (354-540)	471 (387-599)	530 (342-666)	0.91
Missing	1	1	0	
C-reactive protein, mg/L	144 (78-218)	152 (80-218)	121.3 (58.2-238.2)	0.78
Missing	0	0	0	
Lactate, mmol/L	1.52 (1.22-1.91)	1.46 (1.13-1.72)	1.53 (1.25-2.15)	0.30
Missing	3	3	0	
Prothrombin time	1.14 (1.05-1.23)	1.11 (1.05-1.20)	1.18 (1.06-1.25)	0.44
Missing	2	1	1	
PTT	0.97 (0.89-1.04)	0.97 (0.93-1.07)	0.97 (0.89-1.02)	0.46
Missing	2	1	1	

(*continued*)

Table 1 (*continued*)

Characteristics (%)	Overall, n = 55	Without Pulmonary Vascular Thrombosis (n=27)	With Pulmonary Vascular Thrombosis (n=28)	p Value*
D-dimer, μg/mL	3.00 (1.18-18.98)	1.62 (0.93-6.06)	10.06 (1.78-21.00)	0.009
Missing	7	4	3	
Fibrinogen, mg/dL	623 (503-760)	686 (527-773)	594 (451-701)	0.18
Missing	24	13	11	
IL6, pg/mL	74 (38-134)	41.8 (34.8-71.8)	93.6 (48.1-216)	0.02
Missing	17	12	5	
Ferritin, ng/mL	1517 (690-2869)	1130 (748-2479)	1990 (675-3365)	0.22
Missing	9	6	3	
Creatine kinase, U/L	108 (69-212)	115 (75-745)	85 (39-165)	0.09
Missing	11	6	5	
Procalcitonin, ng/mL	0.51 (0.32-1.72)	0.50 (0.34-1.07)	0.95 (0.30-2.29)	0.26
Missing	14	6	8	
Pro-BNP, pg/mL	287 (86-756)	230 (77-747)	490 (156-1121)	0.28
Missing	12	3	9	
Cardiac troponin, ng/L	14.1 (7.07-28.7)	12.4 (7.0-23.8)	15.8 (7.6-44.6)	0.53
Missing	11	4	7	

NOTE. Results reported as median (IQR) or frequency (%).

Abbreviations: ALT, alanine aminotransferase, AST, aspartate transaminase; BMI, body mass index; BNP, brain natriuretic peptide; COPD, chronic obstructive pulmonary disease; COVID-19, coronavirus disease 2019; IQR, interquartile range; M, male; PTT, partial thromboplastin time; WBC, white blood cells.

* P values are calculated by chi-square or Fisher exact test (categorical variables) or Mann Whitney test (continuous variables).

was measured on unenhanced slices; a subsegmental vessel was defined as enlarged when its axial diameter exceeded 3 mm.[17] Imaging after processing was carried out using a commercially available software (Intellispace version 8.0, Philips Medical Systems, Chronic Obstructive Pulmonary Disease tool); after automated identification of pulmonary lobes on unenhanced slices, the software differentiated diverse areas of lung parenchyma based on HU thresholds. In the setting of SARS-CoV-2 pneumonia, the following settings were used: to quantify and differentiate between normal and pathologic lung parenchyma, a -740 HU threshold was set: areas with higher-density values were considered pathologic (disease burden). To distinguish between GGO and non-GGO (crazy paving and/or consolidation) areas, the authors applied a 660-HU threshold.

Descriptor definitions are taken from the *Fleischner Society: Glossary of Terms for Thoracic Imaging*[18]: *Ground-glass opacity* is defined as a hazy increased opacity of lung, with preservation of bronchial and vascular margins; *consolidation* as an opacity of lung that obscures bronchial and vascular margins; and *crazy paving pattern* as thickened interlobular septa and intralobular lines superimposed on a background of GGO, resembling irregularly shaped paving stones.

Software outputs refer to both lungs and single pulmonary lobes as percentages of the overall lung volume. Finally, to accurately assess the precise contribution of GGO and non-GGO patterns to the overall disease burden, the authors calculated the so-called *GGO ratio*, defined as the percentage of pneumonia made up by GGO.

Table 2
Univariate and Multivariate Logistic Regression Models on the Risk of Pulmonary Vascular Thrombosis

Characteristics	Univariate, Odds Ratio (95% Confidence Interval)	p Value	Multivariable, Odds Ratio (95% Confidence Interval)	p Value
Sex (female *v* male)	0.95 (0.29-3.04)	0.93		
Age (continuous)	0.99 (0.95-1.04)	0.91		
COVID-19 symptoms onset, d (continuous)	0.94 (0.88-1.01)	0.10		
Ethnicity (Asian *v* white)	0.10 (0.02-0.93)	0.04		
Hypertension (yes *v* no)	1.12 (0.36-3.40)	0.84		
Absence of anticoagulant prophylaxis before lung thrombosis (yes *v* no)	3.81 (1.21-11.9)	0.02	3.85 (1.01-13.9)	0.04
PO_2/F_IO_2 (continuous)	0.99 (0.95-1.00)	0.73		
Neutro/lympho ratio (continuous)	0.97 (0.91-1.04)	0.43		
Lymphocyte count, $\times 10^9$/L (continuous)	1.04 (0.48-2.24)	0.92		
C-reactive protein, mg/L (continuous)	1 (0.99-1.05)	0.90		
Lactate dehydrogenase, U/L (continuous)	1 (0.99-1.03)	0.70		
D-dimer, μg/mL (continuous)	1.09 (1.01-1.17)	0.02	1.09 (1-1.18)	0.02

Abbreviations: COVID-19, coronavirus disease 2019.

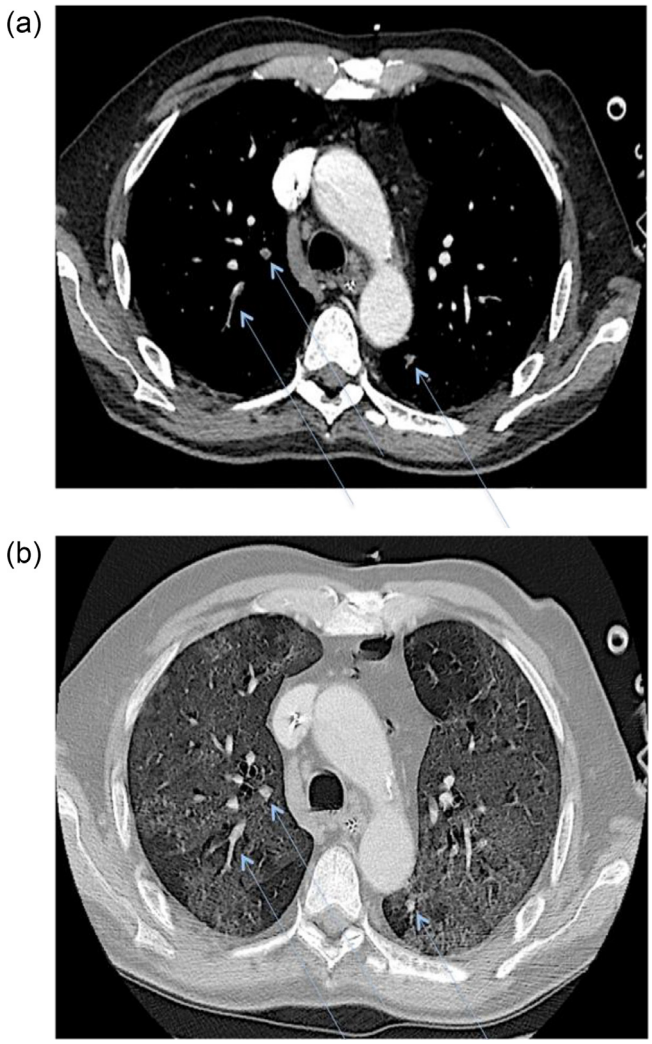

Fig 2. Axial contrast-enhanced CT scan demonstrating simultaneous multiple thrombi with bilateral involvement (A) (*blue arrows*) affecting *sub*segmental pulmonary artery branches within extensive ground-glass opacities (B).

Statistical Analysis

Median values with respective interquartile ranges (IQR) were used to express continuous variables, while frequencies in percentages were used for categorical variables. Patient-related variables and imaging parameters of patients with and without pulmonary vascular thrombosis were compared using the chi-square or Fisher exact test for categorical variables, and the Wilcoxon rank sum or Student *t* test (according to the assessment of normality) for continuous variables. The ability of GGO ratio in predicting the risk of pulmonary vascular thrombosis was determined by the area under the curve of the receiver operating characteristic curve. The optimal cutoff value predicting pulmonary vascular thrombosis was determined on the highest Youden index value (sensitivity + specificity − 1). To evaluate the cutoff accuracy, sensitivity and specificity were estimated. Comparison of GGO values between patients with or without thrombosis was evaluated using a Wilcoxon/Student's *t* test. Univariate and multivariate analyses were used to explore potential risk factors associated with pulmonary vascular thrombosis. The final model included D-dimer level at hospital admission and treatment with anticoagulant before CT pulmonary angiography. A p value of less than 0.05 was considered statistically significant. Statistical analyses were performed with SPSS 25 (SPSS Inc./IBM, Armonk, NY) and R version 3.3.1.

Results

Patient Characteristics

Sixty-seven patients underwent CT pulmonary angiography during the study period. Following exclusions due to severe respiratory and motion artifacts (n = 9) and pneumothorax (n = 3) (Fig 1), 55 patients (39 male [70.9%] with a median age of 62 years [IQR 56-71 years]) were included in this study. Overall, 28 (50.9%) patients showed findings of pulmonary vascular thrombosis at CT pulmonary angiography imaging.

Patient characteristics are summarized in Table 1; most patients had histories of comorbidities, with hypertension being reported in 43.1%. The median time interval between COVID-19 symptom onset and CT pulmonary angiography was 17.5 days (range: 1-38). At the time of CT pulmonary angiography, 27 patients were in COVID-19–dedicated medical wards, 19 in the ICU and nine in the emergency department.

At hospital admission (Table 1), the median values for white blood cell count, lymphocyte count, lactic dehydrogenase, C-reactive protein, serum ferritin, and D-dimer were 9.9 (IQR 6.3-12.3) $\times 10^9$/L, 0.8 (IQR 0.7-1.2) $\times 10^9$/L, 490 (IQR 354-540) U/L, 144 (IQR 78-212) mg/L, 1,517 (IQR 690-2,869) mg/L, and 3 (IQR 1.1-18) μg/mL, respectively. Baseline laboratory findings were not different between patients with or without pulmonary vascular thrombosis, except for D-dimer level (10.06 [1.78-21.00] *v* 1.62 [0.93-6.06]) and IL6 (93.6 [48.1-216] *v* 41.8 [34.8-71.8]), which were increased (p = 0.009 and p = 0.02, respectively) in patients with pulmonary vascular thrombosis.

Laboratory findings at the time of CT pulmonary angiography are summarized in Supplemental Table 1. Before CT pulmonary angiography, 28 patients already were receiving low-molecular-weight heparin or direct thrombin inhibitor (12/28 with and 16/27 without pulmonary vascular thrombosis, p = 0.06).

After a median follow-up of 29.5 (IQR 15-55.7) days after hospital admission, 17 patients died (eight of the patients with and nine of those without pulmonary vascular thrombosis, p = 0.7), 36 were discharged after a median time of 30 (IQR 20-56) days, and two patients were still hospitalized (one with indication of bilateral lung transplantation due to severe fibrosis). Univariate and multivariate analyses are reported in Table 2. An increased level of D-dimer at baseline (odds ratio 1.09, 95% confidence interval 1-1.18, p = 0.02) and absence of anticoagulation before occurrence of pulmonary vascular thrombosis (odds ratio 3.81, 95% confidence interval 1.21-11.9, p = 0.04) were associated independently with the increased risk of pulmonary vascular thrombosis.

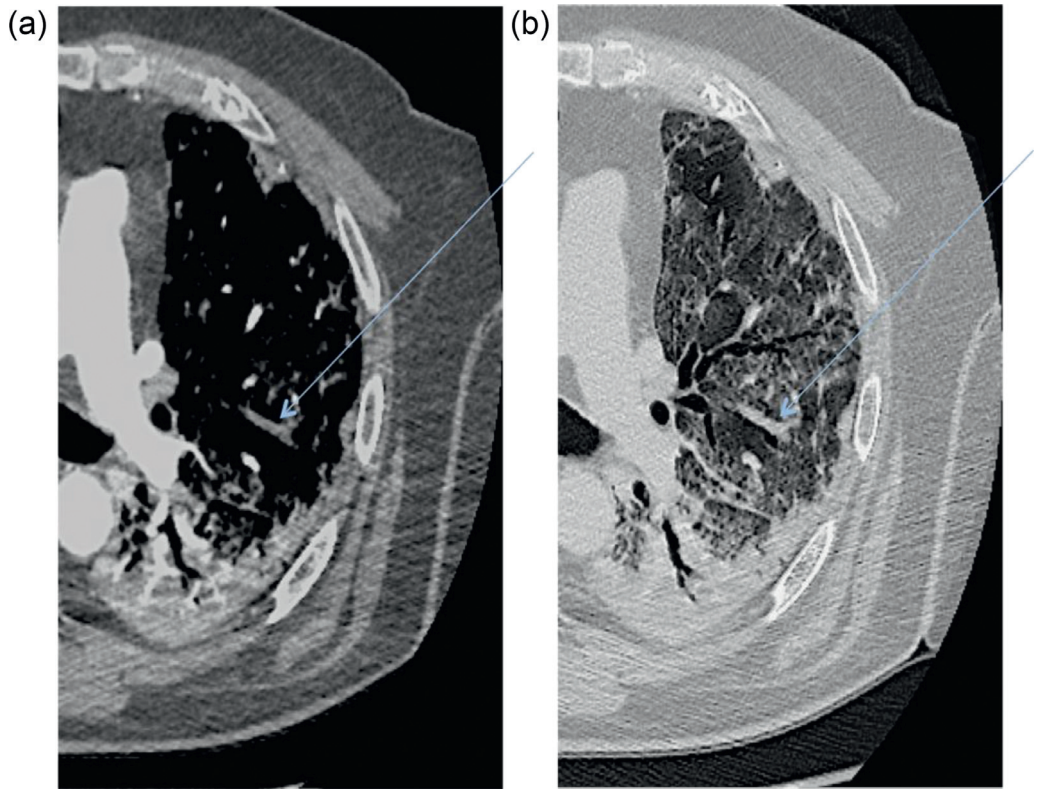

Fig 3. Axial contrast-enhanced CT scan demonstrating a filling defect (A) (*blue arrow*) in the left upper lobe overlapping the segmental distribution of ground-glass opacities (B). Notably, no filling defects are present in the left lower lobe, where consolidation is the main radiologic pattern of pneumonia.

Imaging Findings

Evaluation of Pulmonary Vascular Thrombosis

Simultaneous multiple thromboses were identified in 22 patients (78.6%), with bilateral involvement in 16 of 28 patients (57.1%) (Fig 2). The right lung was the most affected, with the highest involvement in the right lower lobe (18/28, 64.3%), followed by the upper right lobe (17/28, 60.7%) and middle lobe (8/28, 28.6%). The left lung showed involvement in 17 of 28 (60.7%) patients in the lower left lobe and 13 of 28 in the upper left (46.4%).

Filling defects typically were found in segmental (19/28, 67.8%) and subsegmental (27/28 96.4%) branches (Fig 3); lobar branches were affected in only six patients (21.4%).

The presence of an enlarged subsegmental vessel was observed in 31 patients (56.4%, median diameter: 4.2 mm [3-5.7]). Patients with pulmonary vascular thrombosis demonstrated larger subsegmental vessels compared with those without thrombosis (5.25 mm [4.42-6.4] *v* 2.9 mm [2.55-3.2], $p < 0.001$).

Lower and upper limb compression ultrasonography with Doppler evaluation was performed in 27 of 55 patients (12 with and 15 without pulmonary vascular thrombosis). Deep vein thrombosis was detected in four patients (14.8%) (three in the pulmonary vascular thrombosis group, with popliteal and tibial vein thrombosis in one and two patients, respectively).

Pneumonia Evaluation

CT features of SARS-CoV-2 pneumonia are summarized in Table 3. The median disease burden was 74.7% (55.4-83.6); the most affected pulmonary lobes were the lower ones (right: 84.5% [68.35-95.17], left: 88.3% [71.8-95.5]), followed by the upper lobes (right: 67.2% [36.9-85.5], left: 71.9% [35.6-83.9]) and the middle lobe (45.7 [20.6-69.5]). No significant differences were found in disease burden between patients with pulmonary embolism and patients without (73% [33.8-82.4] *v* 75.4% [57.2-85.9] $p = 0.35$). No differences were found even when considering separately right and left lung ($p = 0.26$ and 0.51, respectively) or single pulmonary lobes.

GGOs were present in all patients (55/55, 100%), with a median GGO burden of 22.2% (11.5-36); patients with pulmonary vascular thrombosis had significantly higher GGO areas compared with those without pulmonary vascular thrombosis (31.7% [22.9-41] *v* 17.8% [10.8-22.1] $p < 0.001$). Differences also were found when considering separately right and left lung ($p < 0.001$ in both cases) or single pulmonary lobes. Non-GGO pattern (crazy paving and/or consolidation) was present in 49 of 55 patients (89.1%). GGO ratio analysis also highlighted significant differences between the patients with or without pulmonary vascular thrombosis (57.8% [42.9-71.9] *v* 27.3% [14.5-33.9], $p < 0.001$). Differences also were found when considering separately right and left lung ($p < 0.001$ in both cases) or single pulmonary lobes.

Table 3
Evaluation of Lung Involvement in 55 COVID-19 Patients With Suspected Pulmonary Vascular Thrombosis

	Disease Burden (%)				GGO (%)			GGO Ratio (%)			
	Overall (n = 55)	LT (n = 28)	Non-LT (n = 27)	p Value*	Overall (n = 55)	LT (n = 28)	Non-LT (n=27)	p Value*	Overall (n = 55)	LT (n = 28)	Non-LT (n = 27)	p Value*
Lungs												
Both (RL + LL)	74.75 (55.45-83.57)	73.00 (33.80-82.40)	75.40 (57.20-85.90)	0.35	22.20 (11.50-36.02)	31.70 (22.90-41.00)	17.80 (10.80-22.10)	<0.001	36.88 (23.58-64.79)	57.77 (42.99-71.90)	27.26 (14.50-33.91)	<0.001
RL	72.35 (49.62-81.97)	62.20 (36.90-78.70)	77.70 (53.20-83.50)	0.36	21.50 (13.55-30.55)	30.20 (21.50-41.00)	16.80 (11.60-22.00)	<0.001	39.37 (22.65-65.11)	64.97 (41.03-72.35)	27.46 (17.39-34.69)	<0.001
LL	76.30 (57.67-88.82)	77.20 (36.60-89.50)	75.40 (60.80-88.60)	0.51	20.30 (11.27-31.60)	29.10 (20.10-48.10)	16.20 (8.40-20.70)	<0.001	36.08 (21.76-63.13)	62.31 (46.46-72.90)	24.38 (12.64-33.39)	<0.001
Lobes												
RUL	67.20 (36.87-85.55)	65.50 (28.30-79.00)	71.50 (46.00-86.10)	0.35	23.65 (11.55-32.72)	30.10 (15.00-47.10)	20.30 (10.70-25.60)	<0.001	45.83 (30.77-71.62)	70.75 (50.53-83.75)	34.82 (13.83-44.67)	<0.001
RML	45.70 (20.65-69.55)	31.70 (17.30-59.80)	50.40 (26.00-73.30)	019	16.95 (11.65-29.55)	23.10 (11.80-40.80)	14.20 (11.20-20.10)	<0.001	53.77 (32.20-80.67)	80.21 (72.06-86.15)	37.30 (27.15-52.54)	<0.001
RLL	84.55 (68.35-95.17)	84.20 (59.80-94.40)	87.50 (74.80-96.30)	0.41	19.95 (11.72-31.87)	29.00 (23.20-43.20)	13.80 (8.60-17.80)	<0.001	29.22 (14.59-56.94)	48.10 (31.56-70.47)	15.41 (11.54-24.64)	<0.001
LUL	71.90 (35.62-83.95)	69.60 (26.70-84.40)	74.80 (42.80-80.70)	0.71	21.15 (12.15-40.62)	35.70 (16.30-50.70)	15.50 (10.80-24.60)	<0.001	47.51 (28.77-72.06)	71.88 (53.66-77.80)	35.83 (15.54-47.07)	<0.001
LLL	88.30 (71.80-95.47)	80.70 (53.30-95.30)	89.60 (77.60-96.00)	0.34	19.85 (9.77-31.2)	31.00 (21.60-38.60)	11.70 (5.00 -19.20)	<0.001	29.98 (12.81-49.36)	43.15 (30.11-65.36)	13.41 (8.33-27.99)	<0.001

NOTE. Results reported as frequency (%) and range.
Abbreviations: COVID-19, coronavirus disease 2019; GGO, ground-glass opacities; LL, left lobe; LLL, left lower lobe; LT, lung thrombosis; LUL, left lower lobe; RL, right lobe; RLL, right lower lobe; RML, right middle lobe; RUL, right upper lobe.
* P values are calculated by chi-square or Fisher exact test (categorical variables) or Mann Whitney test (continuous variables).

By means of receiver operating characteristic analysis, the authors identified as best threshold for GGO ratio a percentage of 36.4, above which patients demonstrated a higher risk of pulmonary vascular thrombosis (area under the curve: 0.864; sensitivity: 88.9%; specificity: 85.2%) (Fig 4).

Discussion

This study showed a unique pattern of distribution of pulmonary vascular thrombosis overlapping areas of active GGOs in patients with severe COVID-19 ARDS. Most patients with pulmonary vascular thrombosis showed multiple thrombi (78.6%), with frequent bilateral involvement (57.1%) in segmental and subsegmental pulmonary artery branches, in the presence of larger subsegmental vessels within GGO areas. Furthermore, the authors confirmed an association between D-dimer values and the presence of pulmonary vascular thrombosis.

The percentage of pneumonia characterized by pure GGO (*GGO ratio*) was significantly higher in patients who developed pulmonary vascular thrombosis, with a cutoff, estimated with the receiver operating characteristics analysis, of 36.4%. As a consequence, the results provided the opportunity to define a specific pattern of COVID-19 pneumonia; that is, *GGO predominant*, significantly associated with occurrence of pulmonary vascular thrombosis (Fig 5, central image). Ground-glass opacity is believed to represent the initial, typical response to lung injury, and roughly represents the amount of active inflammation. Furthermore, the observed subsegmental vascular enlargement previously described in SARS-CoV-2 pneumonia[17,19] also has been associated with SARS-CoV-2–triggered hyperemia. The results pointed out a reliable association between subsegmental vascular enlargements within a GGO prevalent pneumonia and the presence of multiple bilateral pulmonary vascular thromboses in the peripheral branches of each lobe artery.

Poissy et al.[20] recently reported a 20.6% pulmonary embolism incidence among the first 107 consecutive patients with COVID-19 admitted to their ICU in France and receiving prophylactic antithrombotic treatment. Grillet et al.[21] also reported that the proportion of patients with acute pulmonary embolism was 23% in the subgroup of 100 patients with COVID-19 infection and severe clinical features (among the 280 hospitalized patients in the study period).

Overall, the current findings confirmed the ability of CT scan to provide a quantitative assessment of the disease severity and confirm the extension of active inflammation as the major determinant of pulmonary vascular thrombosis.[22] Multiple and bilateral pulmonary thromboembolic events already have been reported in patients with COVID-19.[23] However, a systematic topographic analysis of this pattern was lacking and, instead, an embolism concept was proposed; the authors showed stringent pulmonary vascular thrombosis topographic distribution in overlap with GGO areas. Overall, these features supported the concept of an atypical COVID-19-associated ARDS, because the pattern of distribution of pulmonary thromboembolic events in typical ARDS involves areas spared by inflammatory changes.[24] The presence of a high percentage of lung involvement on chest CT has been shown to range

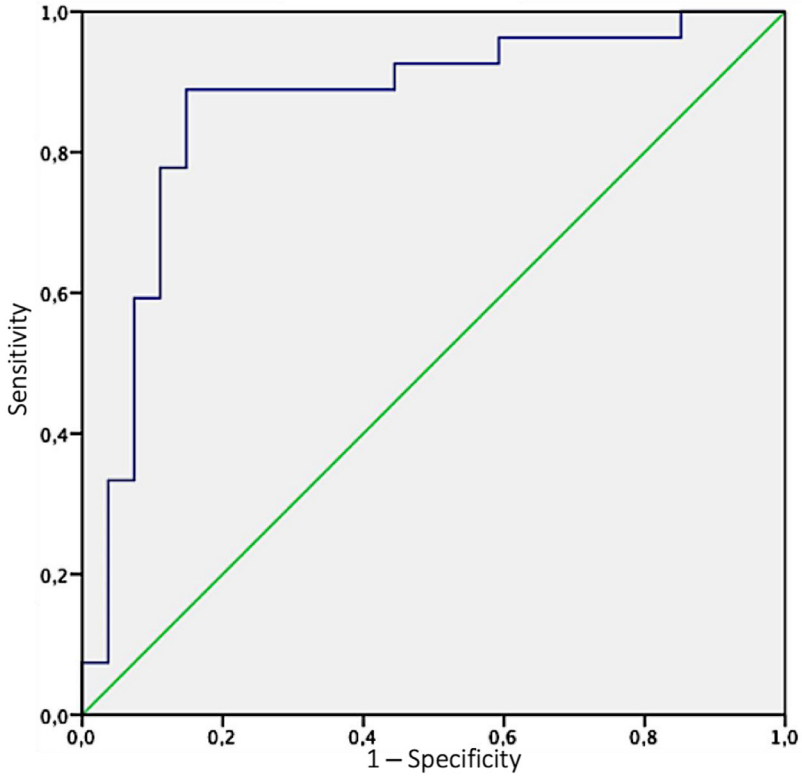

Fig 4. The ability of GGOs (ground-glass opacities) ratio in predicting the risk of pulmonary vascular thrombosis was determined by the area under the curve (AUC) of receiver operating characteristics (ROC) curve; the authors identified as best threshold for GGO ratio a percentage of 36.4, above which patients demonstrated a high risk of pulmonary vascular thrombosis (AUC: 0.864; sensitivity: 88.9%; specificity: 85.2%).

between six and 13 days from symptom onset[10,25]; the median time in pulmonary vascular thrombosis presentation (17.5 days) fits with the hypothesis of an intermediate stage disease,[26] in which lung inflammation is at its highest, resulting in possible progressive endothelial damage. Subsequent activation of the coagulation cascade in the microvascular compartment could lead to a critical functional deterioration of O_2 exchange, ultimately unresponsive to mechanical ventilation.

There is increasing evidence supporting the important role of endothelial cells in the initiation of inflammation and in the development of extensive pulmonary intravascular coagulopathy, which is common in COVID-19 patients with ARDS.[27-29] However, it long has been known that not only diffuse alveolar damage but also pulmonary vascular injury are central pathologic features of ARDS.[30,31] Disregulated inflammation and endothelial cell direct injury promote the expression of coagulation-initiating factors, like tissue factor on cell surfaces, thereby causing downstream activation of coagulation. At the same time, natural anticoagulant mechanisms, including antithrombin, tissue factor pathway inhibitor, and the protein C system, are suppressed and

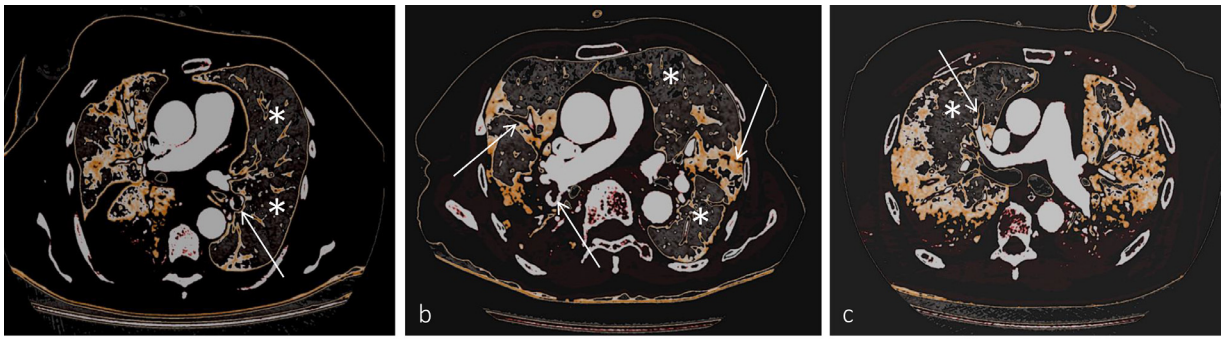

Fig 5. Central image/visual abstract: Computed tomography pulmonary angiography (CTPA) imaging demonstrating, in three different clinical scenarios, eventual filling defects in branches of the pulmonary arteries (*white arrows*) and their spatial distribution according to the corresponding *ventilation maps* (*white asterisks* indicate normal lung parenchyma). In (A) (non-COVID-19 pneumonia) and (C) (non-COVID-19 ARDS) filling defects are electively found in the branches of the pulmonary arteries, accountable for the vascularization of healthy lung segments. On the contrary, in (B) (COVID-19 pneumonia), there is an almost perfect topographical overlap between filling defects distribution and pneumonia extent. COVID-19, coronavirus disease 2019.

this further propagates an uncontrolled cycle of coagulation.[32,33] Other authors suggest that the disruption of pulmonary circulation causes platelet and fibrinogen depletion, suggesting local thrombosis formation.[34]

Histologic postmortem studies revealed diffuse extensive fibrin thrombosis of small and large pulmonary arteries and lung necrosis distal to vascular obstruction in ARDS of diverse etiology.[35-37] Furthermore, bedside balloon occlusion pulmonary angiography demonstrated pulmonary artery filling defects of diverse severity and etiology in about one-half of the patients with ARDS.[35] Severity of the respiratory insufficiency, pulmonary artery pressure, pulmonary vascular resistance, and mortality were significantly higher in patients with angiographic evidence of vascular obstruction than in those with normal angiography.[35] Other authors used the same angiographic technique and found multiple pulmonary artery filling defects in a relevant fraction of patients with severe ARDS.[38]

Overall, even if understanding the role of pulmonary vascular thrombosis in the development of pulmonary hypertension in the course of ARDS is of paramount importance, there still is uncertainty. Besides functional mechanisms, there is evidence of reduced small pulmonary artery diameter by medial artery thickening, and significant reduction in total artery concentration even after short-course ARDS.[39] Because ARDS is a syndrome caused by some primary clinical condition (pneumonia, trauma, shock, sepsis, multiple transfusions, etc.), that could initiate intravascular coagulation; it is not always clear what the main reason is for the observed pulmonary vascular thrombosis in ARDS. The abovementioned studies found a significantly higher rate of thrombotic vascular occlusion in post-traumatic ARDS and in patients with signs of concomitant disseminated intravascular coagulation syndrome.[35,38]

Despite extensive research from the 1970s, the understanding of the basic mechanisms of lung injury and of pulmonary vascular thrombosis in non-COVID-19 ARDS still is uncertain.

As a limitation, the authors acknowledge that this study reported a subset cohort of a larger institutional prospective study. Furthermore, the clinical progression of respiratory distress in this cohort was associated with, but not necessarily caused by, the increased level of D-dimers. On top of this, all consecutive patients undergoing a CT scan for clinical suspicion of pulmonary vascular thrombosis were enrolled; therefore, the overall prevalence in those not presenting clinical suspicion remains unknown. Importantly, in the authors' hospital, deep vein thrombosis[40] was found only in a relatively small percentage of patients with lung thrombosis, and there were no cases in the iliofemoral venous axis, supporting the hypothesis of a lung disease–related complication, due to SARS-CoV2 pathogenicity. The limitation linked to data collected from a single center remains, yet the critical role of the association of disorders in the coagulation pathway, disease severity, and death have been reported in independent cohorts in patients with COVID-19.[4,5,6,41] Acute systemic inflammation features previously have been associated with disease severity and mortality.[8,42] Importantly, D-dimer levels should be considered as an additional predictive tool to stratify patients at risk of adverse outcome and may guide physicians to proceed with CT pulmonary angiography as well as assign anticoagulant administration.

Prospective ongoing randomized trials currently are evaluating the intensity of prophylactic anticoagulation (FREEDOM COVID-19,[43] INHIXACOV19[44]), as well as the use of targeted drugs on endothelium (DEFACOVID,[45] DEFI-VID19[46]). Treatment of COVID-19 pneumonia is changing rapidly with the availability of the results of clinical trials. Immunomodulation therapies to reduce the risk of cytokine- release syndrome induced by SARS-CoV-2 has demonstrated efficacy in single-center and multicenter trials.[47,48]

In conclusion, this study supported the hypothesis of a pathologic relationship between lung inflammation and pulmonary vascular thrombosis, definitively challenging the previous definition of embolism associated with COVID-19 pneumonia and strongly supporting the rationale for an association of anti-inflammatory and anticoagulant treatments in patients with severe COVID-19 pneumonia.

Acknowledgments

The authors are indebted to all healthcare personnel who helped during the COVID-19 emergency.

Conflict of Interest

None.

Supplementary materials

Supplementary material associated with this article can be found in the online version at doi:10.1053/j.jvca.2021.01.011.

References

1 Guan WJ, Ni ZY, Hu Y, et al. Clinical characteristics of coronavirus disease 2019 in China. N Engl J Med 2020;382:1708–20.
2 Ciceri F, Beretta L, Scandroglio AM, et al. Microvascular COVID-19 lung vessels obstructive thromboinflammatory syndrome (MicroCLOTS): An atypical acute respiratory distress syndrome working hypothesis. Crit Care Resusc 2020;22:95–7.
3 Varga Z, Flammer AJ, Steiger P, et al. Endothelial cell infection and endotheliitis in COVID-19. Lancet 2020;395:1417–8.
4 Klok FA, Kruip MJHA, Van der Meer NJM, et al. Incidence of thrombotic complications in critically ill ICU patients with COVID-19. Thromb Res 2020;191:145–7.
5 Kashi M, Jacquin A, Dakhil B, et al. Severe arterial thrombosis associated with Covid-19 infection. Thromb Res 2020;192:75–7.
6 Inciardi RM, Solomon SD, Ridker PM, et al. Coronavirus 2019 disease (COVID-19), systemic inflammation, and cardiovascular disease. J Am Heart Assoc 2020;9:e017756.
7 Cerdà P, Ribas J, Iriarte A, et al. Blood test dynamics in hospitalized COVID-19 patients: Potential utility of D-dimer for pulmonary embolism diagnosis. PLoS One 2020;15:e0243533.
8 Colling ME, Kanti Y. COVID-19-associated coagulopathy: An exploration of mechanisms. Vasc Med 2020;25:471–8.
9 Konstantinides SV, Meyer G, Becattini C, et al. 2019 ESC Guidelines for the diagnosis and management of acute pulmonary embolism developed in collaboration with the European Respiratory Society (ERS): The Task Force for the diagnosis and management of acute pulmonary

embolism of the European Society of Cardiology (ESC). Eur Respir J 2019;54:1901647.
10 Pan F, Ye T, Sun P, et al. Time course of lung changes on chest CT during recovery from 2019 novel coronavirus (COVID-19) pneumonia. Radiology 2020;295:715–21.
11 Ai T, Yang Z, Hou H, Zhan C, et al. Correlation of chest CT and RT-PCR testing for coronavirus disease 2019 (COVID-19) in China: A report of 1014 cases. Radiology 2020;296:E32–40.
12 Rotzinger DC, Beigelman-Aubry C, von Garnier C, et al. Pulmonary embolism in patients with COVID-19: Time to change the paradigm of computed tomography. Thromb Res 2020;190:58–9.
13 Grodecki K, Lin A, Cadet S, et al. Quantitative burden of COVID-19 pneumonia on chest CT predicts adverse outcomes: A post-hoc analysis of a prospective international registry. Radiol Cardiothorac Imaging 2020;2:5.
14 Zangrillo A, Beretta L, Scandroglio AM, et al. Characteristics, treatment, outcomes and cause of death of invasively ventilated patients with COVID-19 ARDS in Milan, Italy. Crit Care Resusc 2020;22:200–11.
15 Zangrillo A, Beretta L, Silvani P, et al. Fast reshaping of intensive care unit facilities in a large metropolitan hospital in Milan, Italy: Facing the COVID-19 pandemic emergency. Crit Care Resusc 2020;1(22):91–4.
16 Rodrigues JCL, Hare SS, Edey A, et al. An update on COVID-19 for the radiologist - A British Society of Thoracic Imaging statement. Clin Radiol 2020;75:323–5.
17 Caruso D, Zerunian M, Polici M, et al. Chest CT features of COVID-19 in Rome, Italy. Radiology 2020;296:E79–85.
18 Hansell DM, Bankier AA, MacMahon H, et al. Fleischner Society: Glossary of terms for thoracic imaging. Radiology 2008;246:697–722.
19 Xie X, Zhong Z, Zhao W, et al. Chest CT for typical coronavirus disease 2019 (COVID-19) pneumonia: Relationship to negative RT-PCR testing. Radiology 2020;296:E41–5.
20 Poissy J, Goutay J, Caplan M, et al. Pulmonary embolism in patients with COVID-19: Awareness of an increased prevalence. Circulation 2020;142:184–6.
21 Grillet F, Behr J, Calame P, et al. Acute pulmonary embolism associated with COVID-19 pneumonia detected with pulmonary CT angiography. Radiology 2020;296:E186–8.
22 Ye Z, Zhang Y, Wang Y, et al. Chest CT manifestations of new coronavirus disease 2019 (COVID-19): A pictorial review. Eur Radiol 2020;30:4381–9.
23 Yang R, Li X, Liu H, Zhen Y, et al. Chest CT severity score: An imaging tool for assessing severe COVID-19. Radiol Cardiothoracic Imaging 2020;2:2.
24 Chiumello D. Acute respiratory distress syndrome (ARDS): Definition, incidence, and outcome. Sham, Switzerland: Springer International Publishing AG; 2017.
25 Hong SB, Kim HJ, Huh JW, et al. A cluster of lung injury associated with home humidifier use: Clinical, radiological and pathological description of a new syndrome. Thorax 2014;69:694–702.
26 Bernheim A, Mei X, Huang M, et al. Chest CT findings in coronavirus disease-19 (COVID-19): Relationship to duration of infection. Radiology 2020;295:200463.
27 McGonagle D, O'Donnell JS, Sharif K, et al. Immune mechanisms of pulmonary intravascular coagulopathy in COVID-19 pneumonia. Lancet Rheumatol 2020;2:e437–45.
28 Teuwen LA, Geldhof V, Pasut A, et al. COVID-19. The vasculature unleashed. Nat Rev Immunol 2020;20:389–91.
29 Cao W, Li T. COVID-19. Towards understanding of pathogenesis. Cell Res 2020;30:367–9.
30 Blaisdell FW. Pathophysiology of the respiratory distress syndrome. Arch Surg 1974;108:44–9.
31 Tomashefski Jr JF, Davies P, Boggis C, et al. The pulmonary vascular lesions of the adult respiratory distress syndrome. Am J Pathol 1983;112:112–26.
32 Opal SM. Interactions between coagulation and inflammation. Scand J Infect Dis 2003;35:545–54.
33 Levi M, van der Poll T. The role of natural anticoagulants in the pathogenesis and management of systemic activation of coagulation and inflammation in critically ill patients. Semin Thromb Hemost 2008;34:459–68.
34 Fraser DD, Patterson EK, Slessarev M, et al. Endothelial injury and glycocalyx degradation in critically ill coronavirus disease 2019 patients: Implications for microvascular platelet aggregation. Crit Care Explor 2020;2:e0194.
35 Greene R, Zapol WM, Snider MT, et al. Early bedside detection of pulmonary vascular occlusion during acute respiratory failure. Am Rev Respir Dis 1981;124:593–601.
36 Zapol WM, Kobayashi K, Snider MT, et al. Vascular obstruction causes pulmonary hypertension in severe acute respiratory failure. Chest 1977;71 (2 suppl):306–7.
37 Hill JD, Ratliff JL, Fallat RJ, et al. Prognostic factors in the treatment of acute respiratory insufficiency with long-term extracorporeal oxygenation. J Thorac Cardiovasc Surg 1974;68:905–17.
38 Vesconi S, Rossi GP, Pesenti A, et al. Pulmonary microthrombosis in severe adult respiratory distress syndrome. Crit Care Med 1988;16:111–3.
39 Snow RL, Davies P, Pontoppidan H, et al. Pulmonary vascular remodeling in adult respiratory distress syndrome. Am Rev Respir Dis 1982;126:887–92.
40 Baccellieri D, Bertoglio L, Apruzzi L, et al. Incidence of deep venous thrombosis in COVID-19 hospitalized patients during the first peak of the Italian outbreak. Phlebology 2020 Nov 26:268355520975592. https://doi.org/10.1177/0268355520975592.
41 Al-Samkari H, Karp Leaf RS, Dzik WH, Carlson JCT, et al. COVID-19 and coagulation: Bleeding and thrombotic manifestations of SARS-CoV2 infection. Blood 2020;136:489–500.
42 Ciceri F, Castagna A, Rovere-Querini P, et al. Early predictors of clinical outcomes of COVID-19 outbreak in Milan, Italy. Clin Immunol 2020;217:108509.
43 FREEDOM COVID-19 anticoagulation strategy (FREEDOM COVID). ClinicalTrials.gov identifier: NCT04512079. Available at: https://clinicaltrials.gov/ct2/show/NCT04512079. Accessed December 30, 2020.
44 Enoxaparin in COVID-19 moderate to severe hospitalized patients (INHIXACOV19). ClinicalTrials.gov identifier: NCT04427098, Available at: https://clinicaltrials.gov/ct2/show/NCT04427098. Accessed December 30, 2020.
45 Defibrotide as prevention and treatment of respiratory distress and cytokine release syndrome of Covid 19 (DEFACOVID). ClinicalTrials.gov identifier: NCT04348383, Available at: https://clinicaltrials.gov/ct2/show/NCT04348383. Accessed December 30, 2020.
46 Defibrotide in COVID-19 pneumonia (DEFI-VID19), ClinicalTrials.gov identifier: NCT04335201 Available at: https://clinicaltrials.gov/ct2/show/NCT04335201. Accessed December 30, 2020.
47 Cavalli G, De Luca G, Campochiaro C, et al. Interleukin-1 blockade with high-dose anakinra in patients with COVID-19, acute respiratory distress syndrome, and hyperinflammation: A retrospective cohort study. Lancet Rheumatol 2020;2:e325–31.
48 Sanders M, Monogue ML, Jodlowski TZ, et al. Pharmacologic treatments for coronavirus disease 2019 (COVID-19): A review. JAMA 2020;323:1824–36.